# Distinguishing Between the Eyes Open and Eyes Closed Brain States Using Permutation Entropy

Christian Dausel Jensen, Julie Timmermann Werge, Laurits Randers, and Stine Byrjalsen
*7th Semester of Mathematical Engineering at Aalborg University*
{cdje20, jwerge20, lrande18, sbyrja20}@student.aau.dk

***Abstract*—Permutation entropy is a method that uses ordinal patterns and can be used to analyse brain activity. In this paper, we utilise ordinal patterns and spatial permutation entropy (SPE) to investigate a method for distinguishing between two brain states: eyes open (EO) and eyes closed (EC). A freely available electroencephalography (EEG) data set consisting of 109 voluntary subjects with EO and EC for 60 seconds each is used to conduct various experiments. The SPE is computed from the ordinal patterns to distinguish between EO and EC. The computation is performed on both unfiltered and filtered data. The EEG data is filtered by isolating the alpha-band frequencies 8-12 Hz, which is acknowledged to capture changes in magnitude for different resting brain states. Furthermore, we experiment with two different permutations of the spatial electrode arrangement. The SPE is calculated for the average of all 109 subjects and for individual subjects. The paired *t*-test is used to quantify the results. To investigate the opportunity for a real-time implementation, we decrease the number of samples. We conclude that the SPE computed from ordinal patterns can be used to distinguish between EO and EC for both average and individual-subject levels. The filter and spatial arrangement of the electrodes influence the possibility of distinguishing between the two brain states using the paired *t*-test. It is found possible to decrease the number of samples and still be able to distinguish between the EO and EC. This potentially enables the usage of real-time applications.**

***Index Terms*—EEG, Ordinal Analysis, Permutation Entropy, Shannon Entropy.**

## I. Introduction

THE human brain is one of the most complex systems in science [10]. Due to its complexity, there is still much to learn about it. To understand the human brain, it is essential to delve into the analysis of brain signals. A useful recording technique for this purpose is electroencephalography (EEG), which involves placing electrodes on the scalp to detect and measure changes in the brain's electrical activity [7].

Investigating and distinguishing between different states in the brain is vital for the early diagnosis of many neurological disorders, such as dementia, epilepsy, and sleep disorders [7] [12]. However, the EEG recordings of brain activity can be influenced by both internal and external factors, such as cognitive processes, emotional states, and environmental noise [7]. These complexities often make it difficult to differentiate between the states of the brain. Therefore, it is crucial to develop precise and robust analytical methods to distinguish between different brain states and identify abnormal patterns that indicate disorders [13]. To address these challenges, one such analytical method is permutation entropy [1]. Permutation entropy is a complexity measure applied to real-valued time series. The Shannon entropy is defined for discrete random variables, therefore, calculating the Shannon entropy directly from a real-valued time series is not possible due to it taking infinitely many values [6, Ch. 2]. Hence, the time series is first transformed into a symbol sequence that takes a finite number of values. This can be done using ordinal patterns, which represent the order of consecutive points in a time series. This method can help reveal information about the transitions in brain activity and may aid in distinguishing between different brain states. Since Bandt and Pompe introduced permutation entropy in their seminal paper in 2002 [1], there has been a rapid increase in its application. Permutation entropy has been used in domains such as detecting epileptic seizures [4], differentiating between brain states under anaesthesia [14], and identifying different sleep stages [15]. Its ability to detect subtle changes in brain activity and its robustness to noise makes it an effective method to investigate state transitions within the brain [15] [1].

To distinguish between different brain states, establishing baseline conditions can be useful. For example, understanding the difference between a subject having eyes open (EO) or eyes closed (EC) can provide a basis for analysing more complex cognitive and neurological conditions [2] [11]. The earliest discovery of occipital alpha-band activity in the brain, associated with the act of opening and closing the eyes, dates back to 1934 [5]. It has since become widely acknowledged that the alpha-band frequencies in EEG, which are between 8-12 Hz, have the highest magnitude when a resting subject has EC, and the alpha-band frequencies are suppressed when the EO [2]. By utilising this knowledge, a recent study on the transition between EO and EC by Boaretto et al. [3] showed that the spatial permutation entropy (SPE), computed from spatial ordinal patterns, could distinguish between EO and EC states. They found that the spatial locations of the electrodes contain valuable information and showed that it is possible to distinguish between brain states. However, a limitation of the previous study is their insufficiency to distinguish between the states at an individual-subject level [3]. Additionally, examining various permutations could lead to an optimal spatial arrangement, significantly increasing the separation between the two states.

In this paper, we will delve into the analysis of EEG signals of the EO and EC states. The aim of this paper is to further develop methods to differentiate between these two states in the brain, using the concepts of ordinal patterns and

SPE. To investigate whether any particular spatial permutation improves the separability of the SPE between the two states, we will examine the permutation from [3] and a permutation of our own design. Furthermore, we want to investigate the possibility of distinguishing between the two states at an individual-subject level. By using fewer samples, we also want to investigate the possibility of real-time implementations since this leads to lower computational complexity and processing time.

The paper is structured as follows: In Section II, the method used for distinguishing between two states in the brain is introduced, along with details about the data set for EO and EC states. In Section III, the results are presented. Finally, the conclusion is given in Section IV.

## II. Methods

### A. Ordinal Patterns

Ordinal patterns transform a real-valued time series $\{x_n\}_{n=1,\dots,N}$ into a symbol sequence $\{s_\ell\}_{\ell=1,\dots,N-D+1}$ that takes values in a finite alphabet $S$ [1]. This is done by first splitting the time series into overlapping segments of length $D$. Each of the $N-D+1$ segments are then assigned an ordinal pattern $\pi = (r_1, r_2, \dots, r_D)$ if $x_{k+r_1} \leq x_{k+r_2} \leq \dots \leq x_{k+r_D}$ where $k$ is the first index of the segment. If $x_{k+l-1} = x_{k+l}$ then $r_{l-1} > r_l$ [12]. There exist $D!$ different ordinal patterns, hence $|S| = D!$ [1]. When $D = 3$, there are $3! = 6$ possible ordinal patterns, which can be seen in Fig. 1.

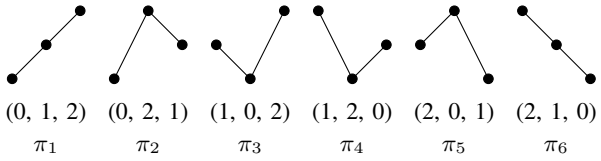


Fig. 1. Illustration of the 6 ordinal patterns for $D = 3$.

The following provides an example of ordinal patterns. Let

$$x = \{9.0, -5.3, 1.7, 1.5, -2.3\}$$

with $D = 3$, which leads to the three segments and their corresponding ordinal patterns

$$\underset{\substack{(1,2,0),\\ \pi_4,}}{\{9.0, -5.3, 1.7\},} \quad \underset{\substack{(0,2,1),\\ \pi_2,}}{\{-5.3, 1.7, 1.5\},} \quad \underset{\substack{(2,1,0).\\ \pi_6.}}{\{1.7, 1.5, -2.3\}.}$$

Hence,

$$s = \{\pi_4, \pi_2, \pi_6\}.$$

### B. Permutation Entropy

The Shannon entropy can be calculated based on the distribution of the ordinal patterns. This is called permutation entropy [1]. To calculate the permutation entropy, the relative frequencies for each permutation must be determined. Given a time series $\{x_n\}_{n=1,\dots,N}$ and its symbol sequence $\{s_\ell\}_{\ell=1,\dots,N-D+1}$ for each permutation $\pi_i$ of length $D$, the relative frequency is defined as

$$p(\pi_i) = \frac{\sum_{j=1}^{N-D+1} \mathbb{1}(s_j = \pi_i)}{N - D + 1},$$

where $\mathbb{1}$ is the indicator function and $i = 1, \dots, D!$ [1]. For a time series consisting of $N$ data points, there are a total of $N - D + 1$ sequences of $D$ points. The distribution of all $D!$ ordinal patterns is referred to as the ordinal distribution. The permutation entropy can then be defined in terms of the relative frequencies. The normalised permutation entropy is

$$H(\boldsymbol{\pi}) = -\frac{1}{\log_2 D!} \sum_{i=1}^{D!} p(\pi_i) \log_2 p(\pi_i),$$

where $\boldsymbol{\pi} = \begin{bmatrix} \pi_1 & \pi_2 & \dots & \pi_{D!} \end{bmatrix}^\top$ [1]. The normalised permutation entropy is maximised and equal to 1 when the ordinal distribution is uniformly distributed [6, Theorem 2.6.4]. Furthermore, it is non-negative [6, Lemma 2.1.1], hence $0 \leq H(\boldsymbol{\pi}) \leq 1$. Henceforth, the normalised permutation entropy will be referred to as the permutation entropy.

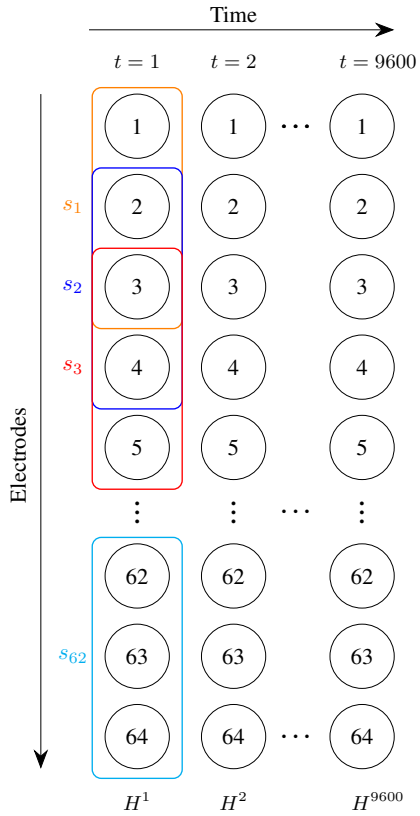


Fig. 3. The approach used to evaluate the SPE [3]. At each time step $t$, the first symbol $s_1$ will be computed from the electrodes (1 2 3), the second $s_2$ from (2 3 4), and so on until the final symbol $s_{62}$ is computed from (62 63 64). With the ordinal patterns, the SPE can be calculated.

### C. Data

We use a freely available data set from [8], [16], [17]. The data set consists of EEG data from 109 voluntary human subjects. For each subject, two 60 seconds EEG recordings were made: one with their EO and one with their EC. The

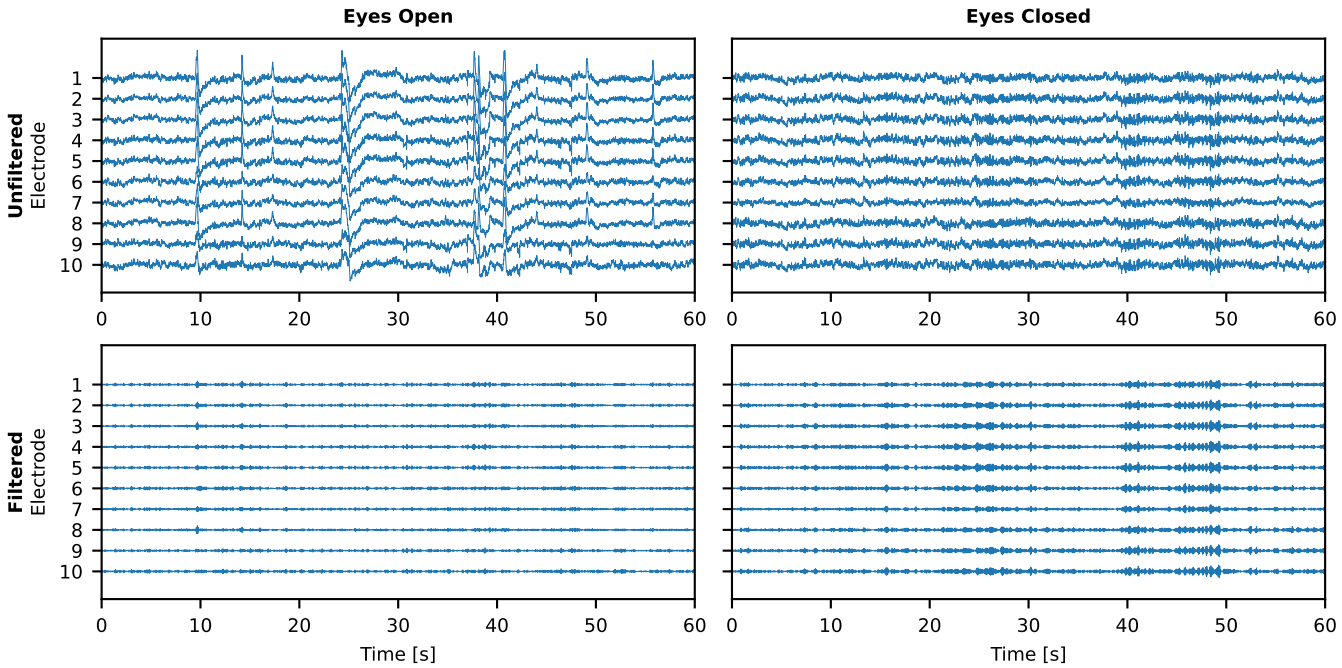


Fig. 2. EEG data for subject 1 with EO and EC. The figure shows both filtered and unfiltered data for 10 electrodes of Permutation 1, see Fig. 4(a).

EEG measurements were performed by 64 scalp electrodes with a sampling rate of 160 Hz, which gives a total of 9600 samples per electrode per recording.

Both unfiltered and filtered time series will be analysed. When filtering, we only consider the alpha-band frequencies, which are 8-12 Hz [3]. In order to isolate the alpha-band, a finite impulse response band-pass filter is designed using the Python library MNE [9]. MNE designs the filter using the window method with a linear phase. The method uses a Hamming window with a filter length of 265. It also compensates for the group delay. An example of unfiltered and filtered data is shown in Fig. 2 for both EO and EC.

### D. Spatial Ordinal Analysis

Assuming the signals recorded by the different electrodes encode valuable spatial information, the ordinal patterns are extracted from the data according to the spatial arrangement of the electrodes. Therefore, the approach to evaluating the SPE can be seen in Fig. 3. We choose $D = 3$ in accordance with [3]. Having 64 electrodes, 62 segments of length 3 are obtained at each time step.

The SPE is denoted $H_i^t$ for the $i$th subject at time $t$. The average SPE over all subjects at time $t$ is

$$\bar{H}^t(\boldsymbol{\pi}) = \frac{1}{M}\sum_{i=1}^{M} H_i^t(\boldsymbol{\pi}), \tag{1}$$

where $M$ is the number of subjects.

## III. Results

Two different spatial arrangements of the electrodes can be seen in Fig. 4(a) and Fig. 4(b). They will be referred to as Permutation 1 and Permutation 2, respectively. In Fig. 5,

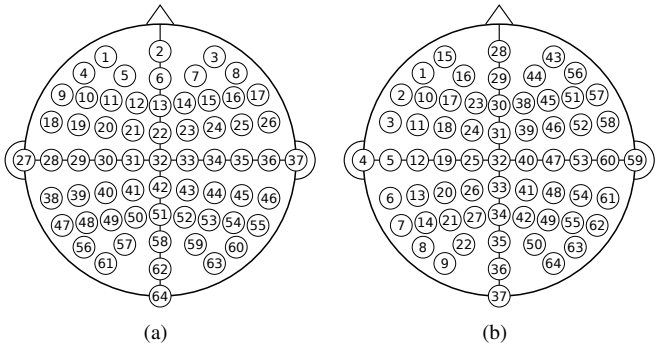


Fig. 4. Two approximate representations of the spatial arrangement of the 64 electrodes on the scalp. (a) The electrodes are arranged from left to right. This permutation is from [3]. (b) The electrodes are arranged from top to bottom.

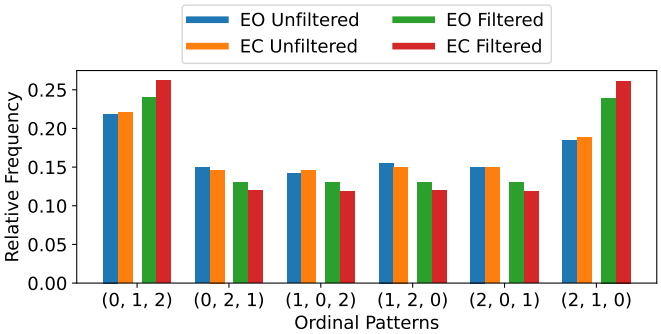


Fig. 5. Subject 3's average ordinal distributions over time for EO and EC states for both unfiltered and filtered data. Permutation 1 from Fig. 4(a) is used.

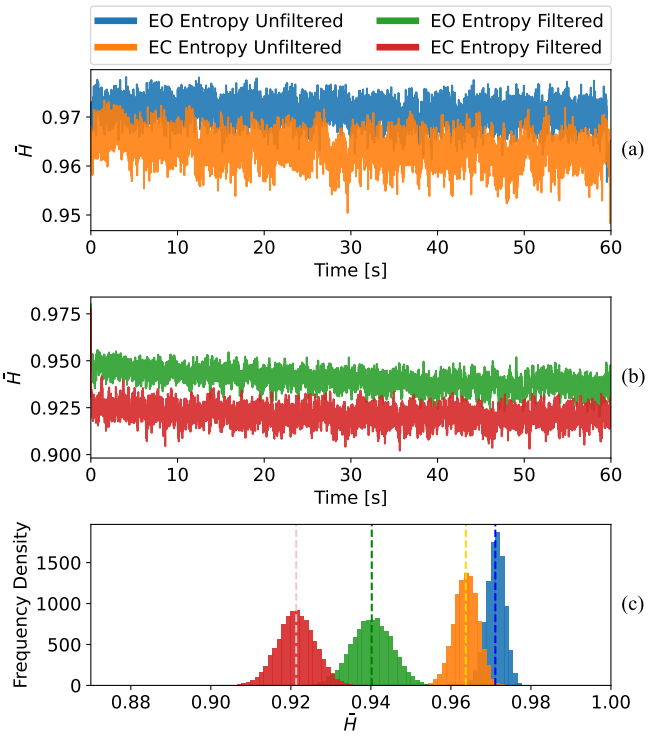


Fig. 6. The average SPE for EO and EC of all 109 subjects for Permutation 1. ((a), (b)) The unfiltered and filtered average SPE of EO and EC over time, respectively. (c) The unfiltered and filtered frequency density of EO and EC from (a) and (b) with a dashed line to represent the mean value of the average SPE.

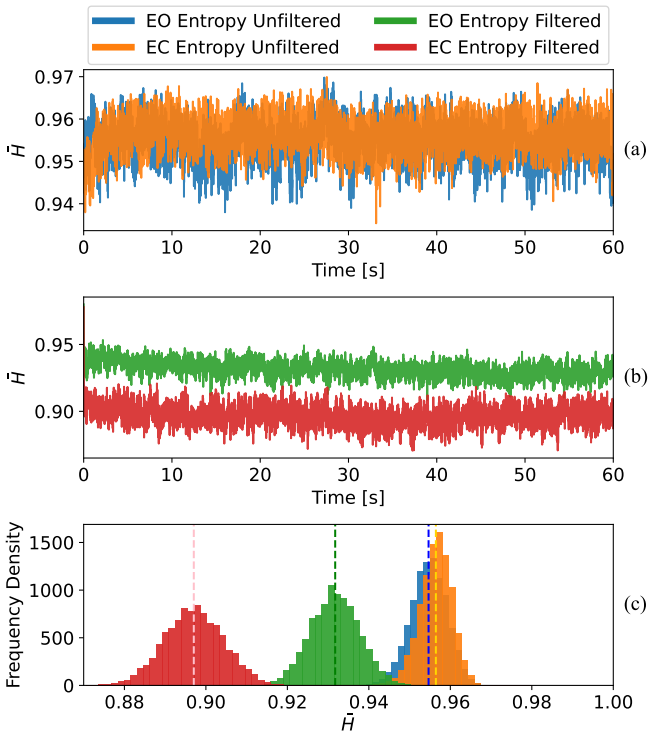


Fig. 7. The average SPE for EO and EC of all 109 subjects for Permutation 2. ((a),(b)) The unfiltered and filtered average SPE of EO and EC over time, respectively. (c) The unfiltered and filtered frequency density of EO and EC from (a) and (b) with a dashed line to represent the mean value of the average SPE.

the average ordinal distributions over time for EO and EC states are shown for both unfiltered and filtered data for subject 3 using Permutation 1. It can be seen that the ordinal distributions differ between the two states, and the difference is greater when the filter is applied.

The average SPE, (1), of the 109 subjects using Permutation 1 is shown in Fig. 6. In Fig. 6(a) and Fig. 6(b), the average SPE for EO and EC over time is shown when the data is unfiltered and filtered, respectively. A histogram of the average SPEs with their corresponding mean values is shown in Fig. 6(c), when the data is both unfiltered and filtered.

It is observed that the average SPE of EO is higher than the average SPE of EC, both for the unfiltered and filtered data. Additionally, when the filter is applied, the difference between the mean values for the average SPE of EO and EC is increased. Generally, the average SPE of EO and EC is lower when the data is filtered.

The same analysis of the average SPE of Permutation 1 in Fig. 6 is illustrated for Permutation 2 in Fig. 7. For the unfiltered data, it is observed that the mean values of the average SPE for EO and EC are very close compared to the mean values of the filtered data. This is illustrated in Fig. 7(c). The average SPE of EO is higher than the average SPE of EC for the filtered data in Fig. 7(b), just as it was observed for Permutation 1 in Fig. 6.

Furthermore, we want to see if it is possible to distinguish between the EO and EC states at an individual-subject level. Therefore, the paired $t$-test is conducted with a significance level of $5\%$. The paired $t$-test compares the mean values obtained from measuring the same population twice under different conditions. It determines whether or not there is a significant difference between the two mean values [18, Ch. 15]. The null hypothesis states that the two mean values of the SPE for EO and EC are equal. This is expressed as

$$H_0 : \mu_{EO} = \mu_{EC}.$$

If the null hypothesis is rejected, we say that it is possible to distinguish between the two states.

Table I presents the results of the paired $t$-test comparing the individual SPEs using Permutation 1 or 2, for both unfiltered and filtered data. The rejection percentages for the null hypothesis are displayed, providing insights into how filtering the data and the spatial arrangement of electrodes influence the individual SPE.

Table I
COMPARISON OF PAIRED $t$-TEST RESULTS FOR THE TWO PERMUTATIONS

| Permutation | Rejection of $H_0$ Unfiltered | Rejection of $H_0$ Filtered |
|---|---|---|
| 1 | 94.50% | 97.25% |
| 2 | 89.90% | 98.17% |

In Table I, it is observed that Permutation 1 has a higher rejection percentage of $H_0$ than Permutation 2 when the

data is unfiltered. However, when applying the filter, both permutations perform fairly even.

We want to investigate how the number of samples influences the paired *t*-test for different combinations of permutation and filtering to evaluate potentially real-time performance. The results can be seen in Table II. The samples are taken from the first part of the signal. The table shows the effect of the number of samples on the rejection percentage of $H_0$ for both Permutation 1 and 2 with filtered and unfiltered data.

Table II
COMPARISON OF REJECTING THE NULL HYPOTHESIS FOR VARIOUS NUMBERS OF SAMPLES

| Number of | Permutation 1 | | Permutation 2 | |
|---|---|---|---|---|
| Samples | Unfiltered | Filtered | Unfiltered | Filtered |
| 800 | 76.14% | 91.74% | 81.65% | 90.82% |
| 640 | 76.14% | 92.66% | 77.98% | 89.90% |
| 480 | 64.22% | 89.90% | 74.31% | 86.23% |
| 320 | 67.88% | 79.81% | 75.22% | 90.82% |
| 160 | 61.46% | 77.98% | 68.80% | 85.32% |
| 80 | 55.04% | 62.38% | 66.05% | 76.14% |
| 40 | 47.70% | 68.80% | 56.88% | 75.22% |

In Table II, the rejection percentage of $H_0$ is generally higher when the data is filtered. The rejection percentage decreases as the number of samples goes down. Additionally, the rejection percentage drops noticeably below 160 samples.

When the data is unfiltered, Permutation 1 has a lower rejection percentage than Permutation 2 for all tested samples. Additionally, Permutation 1 has the largest drop in rejection percentage as the samples go from 800 to 40, corresponding to 5 s and 250 ms.

When the data is filtered, both permutations perform almost equally for 800 to 480 samples. However, below 480 samples, Permutation 1 decreases more sharply than Permutation 2 before reaching 40 samples.

## IV. CONCLUSION

By utilising the average SPE to analyse the EEG signals of the EO and EC states for all subjects, we have found that our approach can distinguish between the two brain states. Our findings correspond with those presented in [3]. However, contrary to the conclusions drawn in [3], we have shown that the SPE of the EO and EC states can be distinguished at the individual-subject level for up to 98.17% of the subjects. This could lead to practical applications in fields such as neurological disorders [2].

To distinguish between the states at the individual-subject level, the paired *t*-test was used. It is important to note that the paired *t*-test does not directly show that a state transition from EO to EC has occurred. It only indicates whether a difference between two mean values is large enough to be considered significant.

To improve the distinction between the EO and EC states and to explore the effect of the electrode spatial arrangement on the SPE, we have investigated two different electrode arrangements. When analysing the unfiltered data, we have found that the spatial arrangements of the electrodes influence how often the paired *t*-test rejects the null hypothesis. Specifically, when the electrodes are arranged from top to bottom in Permutation 2, the mean values are very close for the two states, indicating a weaker distinction. Hence, the electrode arrangement plays a role in the unfiltered data. The choice of the electrode arrangement, however, becomes redundant when the data is filtered and all 9600 samples are used for the analysis.

Filtering the data results in an improved distinction between the EO and EC states, confirming that alpha-band frequencies are related to the act of opening and closing one's eyes [2]. Therefore, employing a finite impulse response band-pass filter can enhance the distinction between the two states. Additionally, for the filtered data, the average SPE is higher during EO states compared to EC states.

In order to investigate the opportunity for a real-time implementation, the number of samples is decreased, leading to a decreased percentage of rejection for the null hypothesis. Despite this decrease, even with 160 samples from the filtered data, it remains possible to distinguish between the states for up to 85.32% of the subjects. This potentially enables the use of real-time applications.


## ACKNOWLEDGEMENT

The authors would like to thank Jan Østergaard and Christophe Biscio for their guidance and feedback throughout the project period.


## REFERENCES


[1] Christoph Bandt and Bernd Pompe. "Permutation Entropy: A Natural Complexity Measure for Time Series". In: *Physical Review Letters* 88.17 (Apr. 11, 2002). Publisher: American Physical Society, p. 174102. DOI: 10.1103/PhysRevLett.88.174102. URL: https://link.aps.org/doi/10.1103/PhysRevLett.88.174102 (visited on 09/06/2023).

[2] Robert J. Barry et al. "EEG differences between eyes-closed and eyes-open resting conditions". In: *Clinical Neurophysiology* 118.12 (Dec. 2007), pp. 2765–2773. ISSN: 13882457. DOI: 10.1016/j.clinph.2007.07.028. URL: https://linkinghub.elsevier.com/retrieve/pii/S1388245707004002 (visited on 11/02/2023).

[3] Bruno R.R. Boaretto et al. "Spatial permutation entropy distinguishes resting brain states". In: *Chaos, Solitons & Fractals* 171 (June 2023), p. 113453. ISSN: 09600779. DOI: 10.1016/j.chaos.2023.113453. URL: https://linkinghub.elsevier.com/retrieve/pii/S0960077923003545 (visited on 09/12/2023).

[4] Angela Bruzzo et al. "Permutation entropy to detect vigilance changes and preictal states from scalp EEG in epileptic patients. A preliminary study". In: *Neurological sciences : official journal of the Italian Neurological Society and of the Italian Society of Clinical Neurophysiology* 29 (Mar. 1, 2008), pp. 3–9. DOI: 10.1007/s10072-008-0851-3.

[5] A. Compston. "The Berger rhythm: potential changes from the occipital lobes in man, by E.D. Adrian and B.H.C. Matthews (From the Physiological Laboratory, Cambridge). Brain 1934: 57; 355-385." In: *Brain* 133.1 (Jan. 1, 2010), pp. 3–6. ISSN: 0006-8950, 1460-2156. DOI: 10.1093/brain/awp324. URL: https://academic.oup.com/brain/article-lookup/doi/10.1093/brain/awp324 (visited on 11/02/2023).

[6] Thomas M. Cover and Joy A. Thomas. *Elements of Information Theory*. John Wiley & Sons, Nov. 28, 2012. 771 pp. ISBN: 978-1-118-58577-1.

[7] Rupak Kumar Das et al. “A Survey on EEG Data Analysis Software”. In: *Sci* 5.2 (June 2023). Number: 2 Publisher: Multidisciplinary Digital Publishing Institute, p. 23. ISSN: 2413-4155. DOI: 10.3390/sci5020023. URL: https://www.mdpi.com/2413-4155/5/2/23 (visited on 10/27/2023).

[8] A. L. Goldberger et al. “PhysioBank, PhysioToolkit, and PhysioNet: components of a new research resource for complex physiologic signals”. In: *Circulation* 101.23 (June 13, 2000), E215–220. ISSN: 1524-4539. DOI: 10.1161/01.cir.101.23.e215.

[9] Alexandre Gramfort et al. “MEG and EEG data analysis with MNE-Python”. In: *Frontiers in Neuroscience* 7 (2013). ISSN: 1662-453X. URL: https://www.frontiersin.org/articles/10.3389/fnins.2013.00267 (visited on 10/06/2023).

[10] Jie Lisa Ji et al. “Mapping the human brain’s cortical-subcortical functional network organization”. In: *NeuroImage* 185 (Jan. 15, 2019), pp. 35–57. ISSN: 1095-9572. DOI: 10.1016/j.neuroimage.2018.10.006.

[11] Gopika Gopan K., Neelam Sinha, and Dinesh Babu J. “Statistical feature analysis for EEG baseline classification: Eyes Open vs Eyes Closed”. In: *2016 IEEE Region 10 Conference (TENCON)*. 2016 IEEE Region 10 Conference (TENCON). ISSN: 2159-3450. Nov. 2016, pp. 2466–2469. DOI: 10.1109/TENCON.2016.7848476. URL: https://ieeexplore.ieee.org/abstract/document/7848476 (visited on 12/06/2023).

[12] Karsten Keller, Anton M. Unakafov, and Valentina A. Unakafova. “Ordinal Patterns, Entropy, and EEG”. In: *Entropy* 16.12 (Dec. 2014), pp. 6212–6239. ISSN: 1099-4300. DOI: 10.3390/e16126212. URL: https://www.mdpi.com/1099-4300/16/12/6212 (visited on 09/06/2023).

[13] Inmaculada Leyva et al. “20 years of ordinal patterns: Perspectives and challenges”. In: *Europhysics Letters* 138.3 (May 2022). Publisher: EDP Sciences, IOP Publishing and Società Italiana di Fisica, p. 31001. ISSN: 0295-5075. DOI: 10.1209/0295-5075/ac6a72. URL: https://dx.doi.org/10.1209/0295-5075/ac6a72 (visited on 09/08/2023).

[14] Duan Li et al. “Multiscale permutation entropy analysis of EEG recordings during sevoflurane anesthesia”. In: *Journal of Neural Engineering* 7.4 (June 2010), p. 046010. ISSN: 1741-2552. DOI: 10.1088/1741-2560/7/4/046010. URL: https://dx.doi.org/10.1088/1741-2560/7/4/046010 (visited on 10/21/2023).

[15] N. Nicolaou and J. Georgiou. “The use of permutation entropy to characterize sleep electroencephalograms”. In: *Clinical EEG and neuroscience* 42.1 (Jan. 2011), pp. 24–28. ISSN: 1550-0594. DOI: 10.1177/155005941104200107.

[16] Gerwin Schalk et al. “BCI2000: a general-purpose brain-computer interface (BCI) system”. In: *IEEE transactions on bio-medical engineering* 51.6 (June 2004), pp. 1034–1043. ISSN: 0018-9294. DOI: 10.1109/TBME.2004.827072.

[17] Gerwin Schalk et al. *EEG Motor Movement/Imagery Dataset*. 2009. DOI: 10.13026/C28G6P. URL: https://physionet.org/content/eegmmidb/ (visited on 09/22/2023).

[18] Robert S. Witte and John S. Witte. *Statistics*. Eleventh edition. Hoboken, NJ: Wiley, 2017. 480 pp. ISBN: 978-1-119-25451-5.